# A DIRECT METHOD FOR THE DESIGN OF 2-D NONSEPARABLE FILTER BANKS

*W.-S. Lu, A. Antoniou, and H. Xu*

Dept. of Electrical and Computer Engineering
University of Victoria
Victoria, B.C., Canada, V8W 3P6
Phone: 721-8781, FAX: (604)721-6052, email: andreas@ece.uvic.ca

## ABSTRACT

A direct approach for the design of 2-D nonseparable diamond-shaped filter banks is proposed. The design goal is achieved by formulating the problem as an iterative quadratic programming problem in which the perfect reconstruction condition is incorporated into a weighted least squares type objective function while satisfactory stopband attenuation is assured by imposing a set of constraints on the amplitude of the lowpass analysis filter in the stopband. Analytical formulas for the exact and efficient evaluation of the objective function are derived, and an analysis on the local convergence of the proposed algorithm is given. The paper concludes with two design examples that illustrate the proposed design method.

## 1. INTRODUCTION

One of the important classes of two-dimensional (2-D) filter banks is the class of nonseparable diamond-shaped filter banks [1][2]. A lowpass 2-D filter with diamond-shaped passband retains significant horizontal as well as vertical frequency components while rejecting less important diagonal frequency components. Filter banks of this type have been applied to image and video compression and HDTV with satisfactory results [3]. Many existing methods for the design of 2-D nonseparable filter banks are based on the application transformations to one-dimensional (1-D) prototype filters [3], [5]–[7], and are referred to as indirect methods here. In [8], a direct method for the design of 2-D nonseparable filter banks by using linear programming is described.

The purpose of this paper is to propose a new direct approach for the design of 2-D nonseparable diamond-shaped filter banks. To achieve reconstruction and intra-band error minimization, we employ an objective function which is a weighted sum of two error components. This objective function turns out to be a fourth-order function of the filter coefficients. Constraints on maximum ripple in the stopband of the lowpass analysis filter are imposed to achieve satisfactory stopband attenuation. To solve this nonlinear constrained optimization problem efficiently, a technique similar to one used in 1-D filter bank designs [9]–[11] is used to modify the objective function into a quadratic function with positive definite Hessian matrix. Furthermore, analytic formulas are derived to evaluate the terms involved in the modified objective function. These formulas result in precise and efficient function evaluations as compared to summing up a large number of discretized terms which would be time consuming and inevitably introduce additional errors into the design. As a result, the design problem at hand is reduced to an iterative quadratic programming problem which can be solved by using, for example, the active set method [12]. A quantitative analysis on local convergence of the proposed design algorithm is given. Two examples are given to illustrate the design method proposed and to compare it with the unconstrained least squares design.

## 2. PROPOSED DESIGN METHOD

### 2.1. Formulation of the objective function

A 2-D nonseparable diamond-shaped filter bank can be represented by the system shown in Fig. 1. The ideal frequency response of the analysis lowpass filter $H_0$ is depicted in Fig. 2. After filtering by the analysis filters, the signals are quincunx downsampled. At the reconstruction end, the signals are upsampled with the discarded samples replaced by zero values. Analytically the input and output relationship of the filter bank can be expressed as

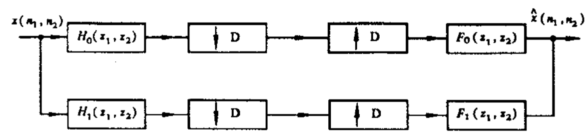


Fig. 1 2-D diamond-shaped filter bank system.

$$\begin{aligned}\hat{X}(z_1, z_2) &= \tfrac{1}{2}[H_0(z_1, z_2)F_0(z_1, z_2) + H_1(z_1, z_2)F_1(z_1, z_2)] \\ &\cdot X(z_1, z_2) + \tfrac{1}{2}[H_0(-z_1, -z_2)F_0(z_1, z_2) \\ &+ H_1(-z_1, -z_2)F_1(z_1, z_2)] \cdot X(-z_1, -z_2) \quad (1)\end{aligned}$$

where the first term represents the input signal component and the second term represents the aliasing component. By assuming that

$$H_1(z_1, z_2) = z_1^{-1} H_0(-z_1, -z_2) \quad (2a)$$
$$F_0(z_1, z_2) = H_0(z_1, z_2) \quad (2b)$$
$$F_1(z_1, z_2) = z_1 H_0(-z_1, -z_2) \quad (2c)$$

the aliasing term in Eqn. (1) is canceled and (1) becomes

$$\hat{X}(z_1, z_2) = \left[H_0^2(z_1, z_2) + H_0^2(-z_1, -z_2)\right] \cdot X(z_1, z_2) \quad (3)$$

So if the condition

$$H_0^2(\omega_1, \omega_2) + H_0^2(\omega_1 + \pi, \omega_2 + \pi) = 1 \quad (4)$$

is satisfied, then the output will be a replica of the input.

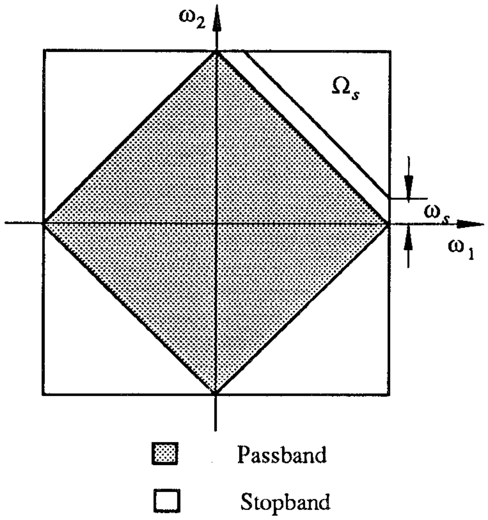


Fig. 2 Band characteristics.

Assuming that the region of support of filter $H_0$ is a $(2N_1-1)\times(2N_2-1)$ rectangle centered at the origin of the $(n_1, n_2)$ plane and its impulse response $h(n_1, n_2)$ for $n_1 = -(N_1-1), \ldots, N_1-1$ and $n_2 = -(N_2-1), \ldots, N_2-1$, is of quadrantal symmetry, then the frequency response of filter $H_0$ can be expressed as [13]

$$\begin{aligned} H_0(\omega_1, \omega_2) &= \sum_{n_1=0}^{N_1-1}\sum_{n_2=0}^{N_2-1} a(n_1, n_2)\cos(n_1\omega_1)\cos(n_2\omega_2) \\ &= \mathbf{h}^T\mathbf{c}(\omega_1, \omega_2) \end{aligned} \tag{5}$$

where

$$\begin{aligned} \mathbf{h} = [\ &a(0,0)\ a(1,0)\ \ldots\ a(N_1-1,0)\ a(0,1) \\ &\ldots\ a(N_1-1,1)\ \ldots a(N_1-1, N_2-1)]^T \end{aligned}$$

is a column vector formed by reordering $a(n_1, n_2)$; on the other hand, $\mathbf{c}(\omega_1, \omega_2)$ is a column vector whose $i$th entry can be expressed as

$$\begin{aligned} c(i) &= \cos p(i)\omega_2 \cdot \cos q(i)\omega_1,\ \ p(i) = \operatorname{int}\left[\frac{i-1}{N_1}\right] \\ q(i) &= i - 1 - \operatorname{int}\left[\frac{i-1}{N_1}\right]\cdot N_1 \end{aligned}$$

As for the 1-D case, there are two requirements for a 2-D analysis/synthesis system, namely, reconstruction error and intra-band aliasing minimization. To satisfy these requirements, an objective function can be formed as

$$E = E_1 + \alpha E_2 \tag{6}$$

where $\alpha > 0$ is a weight and the first term $E_1$, defined as

$$E_1 = \int_0^\pi\int_0^\pi \left[H_0^2(\omega_1, \omega_2) + H_0^2(\omega_1+\pi, \omega_2+\pi) - 1\right]^2 d\omega_1 d\omega_2$$

is used to approximate perfect reconstruction and the second error component $E_2$, defined as

$$E_2 = \iint_{\Omega_s} H_0^2(\omega_1, \omega_2)\, d\omega_1 d\omega_2$$

is used to reduce intra-band aliasing. The region of integration $\Omega_s$ is the upper part of the first quadrant in Fig. 2, which corresponds to the stopband of $H_0$.

### 2.2. Constraints on $G_0(z_1, z_2)$

The weight $\alpha$ in (6) can be adjusted to satisfy the desired reconstruction accuracy. As a result, however, the maximum ripple in the stopband of $G_0(z_1, z_2)$ usually would increase. In order to achieve a satisfactory stopband attenuation in $G_0(z_1, z_2)$, we impose the constraints

$$|G_0(e^{j\omega_1}, e^{j\omega_2})| \le \delta_s \quad \text{for} \quad (\omega_1, \omega_2) \in \hat{\Omega}_s \tag{7}$$

where $\hat{\Omega}_s$ denotes a discrete set of sampling points in region $\Omega_s$, and $\delta_s$ is the maximum ripple allowed in the stopband of $G_0(z_1, z_2)$. If $\hat{\Omega}_s$ contains $K$ points $(\omega_{1i}, \omega_{2i})$, $1 \le i \le K$, then the $2K$ constrains (7) can be expressed in matrix notation as

$$\mathbf{Cg} \le \delta_s\mathbf{e} \tag{8}$$

where

$$\mathbf{C} = \begin{bmatrix} \mathbf{c}^T(\omega_{11}, \omega_{21}) \\ -\mathbf{c}^T(\omega_{11}, \omega_{21}) \\ \vdots \\ \mathbf{c}^T(\omega_{1K}, \omega_{2K}) \\ -\mathbf{c}^T(\omega_{1K}, \omega_{2K}) \end{bmatrix}_{2K\times N_1N_2}, \quad \mathbf{e} = \begin{bmatrix} 1 \\ 1 \\ \vdots \\ 1 \\ 1 \end{bmatrix}_{2K\times 1} \tag{9}$$

### 2.3. Iterative Linearization Technique

The minimization of $E$ in (6) with respect to the coefficients in $\mathbf{h}$ subject to constraints (8) with conventional constrained optimization methods is time-consuming because of the high nonlineararity of $E$. Here we use an iterative method in which the error function $E$ in (6) is modified as

$$E' = E_1' + \alpha E_2' \tag{10}$$

where

$$\begin{aligned} E_1' &= \int_0^\pi\int_0^\pi [H_0(\omega_1, \omega_2)G_0(\omega_1, \omega_2) + H_0(\omega_1+\pi, \omega_2+\pi) \\ &\quad \cdot G_0(\omega_1+\pi, \omega_2+\pi) - 1]^2\, d\omega_1\, d\omega_2 \\ E_2' &= \iint_{\Omega_s} G_0^2(\omega)\, d\omega_1\, d\omega_2 \end{aligned}$$

Like $H_0$, filter $G_0$ is a lowpass FIR filter of the same order with quadrantally symmetrical impulse response, and frequency response $G_0(\omega_1, \omega_2) = \mathbf{g}^T\mathbf{c}(\omega_1, \omega_2)$ where $\mathbf{g}$ is a column vector whose elements are the values of impulse response of $G_0$. To start the iteration, we design a 2-D diamond-shaped lowpass filter by a conventional 2-D FIR filter design method [13], and use its coefficients to form the initial $\mathbf{h}$. After extensive manipulations, it can be shown that $E'$ in (10) can be written in terms of a quadratic form of $\mathbf{g}$ as

$$E' = \mathbf{g}^T(\mathbf{U} + \alpha\mathbf{U}_s)\mathbf{g} - 2\mathbf{h}^T\mathbf{B}\mathbf{g} + \pi^2 \tag{11}$$

where $B = (b_{ij})$ with

$$\begin{aligned} b_{ij} &= \frac{\pi^2}{2}\{\delta[p(i)+p(j)] + \delta[p(i)-p(j)]\} \\ &\quad \cdot\{\delta[q(i)+q(j)] + \delta[q(i)-q(j)]\} \end{aligned} \tag{12a}$$

where $\delta(k)$ is the unit impulse and $\mathbf{U} = (u_{ij})$ with

$$u_{ij} = 2 \sum_{n_1=0}^{N_1-1} \sum_{n_2=0}^{N_2-1} \sum_{m_1=0}^{N_1-1} \sum_{n_2=0}^{N_2-1} h(n_1, n_2) h(m_1, m_2) \left[1 + (-1)^{m_1+m_2+p(j)+q(j)}\right] \cdot I[n_1, m_1, q(i), q(j)]\, I[n_2, m_2, p(i), p(j)] \quad (12b)$$

$$I(n_1, n_2, n_3, n_4) = \int_0^{\pi} \cos n_1\omega \cos n_2\omega \cos n_3\omega \cos n_4\omega \, d\omega \quad (12c)$$

Next, we note that $E_2' = \mathbf{g}^T \mathbf{U}_s \mathbf{g}$ with

$$\mathbf{U}_s = \int_{\omega_s}^{\pi} d\omega_2 \int_{\pi-(\omega_2-\omega_s)}^{\pi} \mathbf{c}(\omega_1, \omega_2)\mathbf{c}^T(\omega_1, \omega_2)\, d\omega_1 \quad (12d)$$

where $\omega_s$ is the stopband edge.

Since $\mathbf{U}^T\mathbf{U} + \alpha \mathbf{U}_s^T \mathbf{U}_s$ is positive definite, $E'$ is strictly globally convex quadratic function, and minimizing $E'$ subject to constraints (8) is a typical *quadratic programming* (QP) problem which can be solved effectively by using the active set method [12]. Having obtained $\mathbf{g}$, a linear formula can be used to update $\mathbf{h}$ as

$$\mathbf{h} := (1-\tau)\mathbf{h} + \tau\mathbf{g} \quad (13)$$

where $0 < \tau < 1$ is called the smoothing parameter. The above process is repeated until $\| \mathbf{h} - \mathbf{g} \|$ is less than a prescribed tolerance.

The design procedure can now be summarized in terms of the following algorithm:

**Algorithm**

**Step 1** Use a conventional method (e.g., the singular-value decomposition method) to design a 2-D, $(2N_1 - 1) \times (2N_2 - 1)$ diamond-shaped FIR filter and use its impulse response to form the initial $\mathbf{h}$.

**Step 2** Calculate $\mathbf{B}$ and $\mathbf{U}_s$ using (12a) and (12d), respectively.

**Step 3** Use (12b) to form $\mathbf{U}$ and solve the QP problem.

Minimize $E' = \mathbf{g}^T(\mathbf{U} + \alpha\mathbf{U}_s)\mathbf{g} - 2\mathbf{h}^T\mathbf{B}\mathbf{g} + \pi^2$ (14a)

Subject to $\mathbf{C}\mathbf{g} \leq \delta_s \mathbf{e}$ (14b)

for $\mathbf{g}$.

**Step 4** If $\| \mathbf{h} - \mathbf{g} \| < \epsilon$, where $\epsilon$ is a prescribed tolerance, output $\mathbf{g}$ as the design result and stop. Otherwise, update $\mathbf{h}$ using (13) and repeat from Step 3.

It is worthwhile to note that matrices $\mathbf{B}$ and $\mathbf{U}_s$ can be pre-calculated as soon as $N_1$, $N_2$, and $\omega_s$ are determined. In addition, the integrals involved in determining the entries of $\mathbf{U}$ can be pre-calculated and stored as a table which can be loaded for use when the iteration starts. Note also that $\mathbf{B}, \mathbf{U}_s$, and $\mathbf{U}$ are all symmetrical matrices and, therefore, only about half of their entries need to be computed. The smoothing parameter $\tau$ is in the range of $(0, 1)$. Our numerical experiments indicate that the value of $\tau$ around 0.5 leads to fast convergence.

### 2.4. Convergence Analysis

Because of the high degree of nonlinearity of the QP problem with respect to vector $\mathbf{h}$, a general convergence analysis on the algorithm is fairly difficult. In what follows, we derive a sufficient condition under which local convergence of the algorithm is guaranteed.

Denote the vector $\mathbf{h}$ obtained after $k$ iterations by $\mathbf{h}_k$ and the vector $\mathbf{g}$ obtained from the quadratic programming

Minimize $\mathbf{g}^T(\mathbf{U}^{(k)} + \alpha\mathbf{U}_s)\mathbf{g} - 2\mathbf{h}_k^T\mathbf{B}\mathbf{g} + \pi^2$ (15a)

Subject to $\mathbf{C}\mathbf{g} \leq \delta_s \mathbf{e}$ (15b)

by $\mathbf{g}_k$, where $\mathbf{U}^{(k)}$ is the matrix $\mathbf{U}$ defined in (12) with $\mathbf{h}$ replaced by $\mathbf{h}_k$. For notation simplicity, we use $\mathbf{g}_k = T(\mathbf{h}_k)$ to describe the solution of (15) for a given $\mathbf{h}_k$. It now follows that (13) can be written as

$$\mathbf{h}_{k+1} = F(\mathbf{h}_k) \quad \text{for } k = 0, 1, \ldots \quad (16a)$$

where

$$F(\mathbf{h}_k) = (1-\tau)\mathbf{h}_k + \tau T(\mathbf{h}_k) \quad (16b)$$

From (16a) we see that if the sequence $\{\mathbf{h}_k, \ k = 0, 1, \ldots\}$ converges to a vector, say $\mathbf{h}^*$, then $\mathbf{h}^*$ is a *fixed point* of function $F$, i.e., $F(\mathbf{h}^*) = \mathbf{h}^*$. It is known [14] that the sequence $\mathbf{h}^*$ generated by (16) converges locally to a fixed point of $F$ if at $\mathbf{h} = \mathbf{h}^*$

$$\left\| \frac{\partial F}{\partial \mathbf{h}} \right\|_2 \leq \beta < 1 \quad (17)$$

Here $\partial F / \partial \mathbf{h}$ denotes the Jacobian of $F$ with respect to $\mathbf{h}$, and the term "local convergence" is referred to the convergence of $\{\mathbf{h}_k\}$ with the initial point $\mathbf{h}_0$ in a certain neighborhood of $\mathbf{h}^*$. It follows from (16b) that

$$\left\| \frac{\partial F}{\partial \mathbf{h}} \right\|_2 \leq (1-\tau) + \tau \left\| \frac{\partial T}{\partial \mathbf{h}} \right\|_2$$

Hence (17) holds if

$$\left\| \frac{\partial T}{\partial \mathbf{h}} \right\|_2 \leq \beta < 1 \quad \text{at } \mathbf{h} = \mathbf{h}^* \quad (18)$$

In order to ensure that the initial $\mathbf{h}_0$ is in a small vicinity of $\mathbf{h}^*$, one can apply a conventional method such as the window method or the SVD method [15] to design a diamond-shaped, lowpass, linear-phase, FIR 2-D filter and then use the filter coefficients obtained to form the vector $\mathbf{h}_0$.

An alternative sufficient condition for the convergence of $\{\mathbf{h}_k, \ k = 0, 1, \ldots\}$ is the existence of a constant $\beta < 1$ and a positive integer $K$ such that

$$\|F(\mathbf{h}_k) - F(\mathbf{h}_{k-1})\| \leq \beta \|\mathbf{h}_k - h_{k-1}\| \quad (19)$$

for all $k \geq K$. The reason why (19) assures the convergence of $\{\mathbf{h}_k\}$ is that from (19) we have for $k \geq K$

$$\begin{aligned} \|F(\mathbf{h}_k) - F(\mathbf{h}_{k-1})\| &\leq \beta \|F(\mathbf{h}_{k-1}) - F(\mathbf{h}_{k-2})\| \\ &\leq \beta^{k-K+1} \|\mathbf{h}_K - \mathbf{h}_{K-1}\| \end{aligned}$$

It follows that for sufficiently large integers $m > n \geq K$

$$\begin{aligned} \|\mathbf{h}_m - \mathbf{h}_n\| &\leq \sum_{l=0}^{m-n-1} \|\mathbf{h}_{n+l-1} - \mathbf{h}_{n+l}\| \\ &\leq \frac{\beta(\beta^{n-K} - \beta^{m-K})}{1-\beta} \|\mathbf{h}_K - \mathbf{h}_{K-1}\| \end{aligned}$$

which approaches zero when $m$ and $n$ tend to infinity. Hence $\{\mathbf{h}_k\}$ is a Cauchy sequence whose convergence is guaranteed.

## 3. DESIGN EXAMPLES

We now present two design examples to illustrate the proposed algorithm. The design specifications were $N_1 = N_2 = 8$, $\alpha = 0.001$, $\tau = 0.5$, $\omega_s = 1.2$, $\delta_s = 0.016$, $\epsilon = 10^{-3}$ for Example 1; and $N_1 = N_2 = 9$, $\alpha = 0.001$, $\tau = 0.5$, $\omega_s = 1.2$, $\delta_s = 0.01$, $\epsilon = 10^{-3}$ for Example 2. The perfect reconstruction performance of the filter banks obtained was evaluated in terms of the peak reconstruction error

$$\text{PRE} = \max_{\omega_1, \omega_2} |20 \log_{10} [H_0^2(\omega_1, \omega_2) + H_0^2(\omega_1 + \pi, \omega_2 + \pi)]|$$

The stopband attenuation of the individual filters was evaluated in terms of minimum stopband attenuation

$$\text{MSA} = \min_{\omega_1, \omega_2 \in \Omega_s} [-20 \log_{10} |H_0(\omega_1, \omega_2)|]$$

To compare the results obtained with constraints (14b) with those obtained without (14b), the designs were first carried out by applying the algorithm described in Sec. 2.3. The constraints in (14b) were formulated on set $\hat{\Omega}_s$ consisting of 15 points evenly placed in the region $\Omega_s$ (see Figure 2). The results are listed in the upper portion of Table 1. Next, Step 3 of the algorithm was modified by dropping the constraints in (14b). In this case, vector g that minimizes (14a) is given by

$$\mathbf{g} = (\mathbf{U} + \alpha \mathbf{U}_s)^{-1} \mathbf{B} \mathbf{h}$$

The modified algorithm was applied to design two filter banks with the same sets of specifications. The results obtained are listed in the lower portion of Table 1. It is observed that QP with constraints (14b) indeed improves the stopband attenuation compared to its counterpart obtained by the weighted least squares design at the expense of slight increase in PRE. As is shown in Table 1, the algorithm converges after 15 and 21 iterations for Example 1 and 2, respectively. The coefficient matrix of the filter $H_0$ designed in Example 1, $(a_{ij})$, using constrained optimization is given in Table 2.

Table 1: Performance evaluations of obtained filter banks

| | | Example 1 | Example 2 |
|---|---|---|---|
| with Constraints (14b) | Iterations | 11 | 19 |
| | PRE (dB) | $3.9210 \times 10^{-4}$ | $2.4852 \times 10^{-4}$ |
| | NSA (dB) | 40.6129 | 44.2448 |
| without constraints (14b) | Iterations | 13 | 10 |
| | PRE (dB) | $3.6362 \times 10^{-4}$ | $1.7251 \times 10^{-4}$ |
| | MSA (dB) | 31.1483 | 34.4826 |

Table 2: Coefficients of $H_0(z_1, z_2)$ in Example 1

| Columns 1 through 4 | | | |
|---|---|---|---|
| 5.7235e−1 | 3.8013e−1 | −1.1880e−2 | 2.3324e−2 |
| 3.7988e−1 | −1.1762e−1 | −1.9396e−1 | 1.8019e−2 |
| −1.1849e−2 | −1.9369e−1 | 8.5242e−2 | 6.4846e−2 |
| 2.3270e−2 | 1.7964e−2 | 6.4696e−2 | −4.6702e−2 |
| −6.8743e−3 | −1.2676e−2 | −1.1435e−2 | −1.6421e−2 |
| 6.7193e−4 | 7.8494e−3 | 2.2964e−3 | 4.9182e−3 |
| −1.4176e−3 | −8.6153e−5 | −2.6078e−3 | −1.8383e−4 |
| −3.6861e−4 | 1.1834e−3 | −3.0345e−4 | 3.7920e−4 |

| Columns 5 through 8 | | | |
|---|---|---|---|
| −6.8936e−3 | 6.7678e−4 | −1.4256e−3 | −3.7113e−4 |
| −1.2724e−2 | 7.8805e−3 | −8.5461e−5 | 1.1921e−3 |
| −1.1485e−2 | 2.3101e−3 | −2.6247e−3 | −3.0782e−4 |
| −1.6479e−2 | 4.9487e−3 | −1.8447e−4 | 3.8562e−4 |
| 1.7513e−2 | 1.7962e−3 | −9.9789e−4 | 2.5360e−4 |
| 1.7882e−3 | −2.8779e−3 | −7.7403e−5 | −3.0128e−4 |
| −9.8892e−4 | −7.8655e−5 | −5.1124e−4 | 4.9422e−4 |
| 2.5474e−4 | −3.0085e−4 | 4.9265e−4 | −5.1892e−5 |


### Acknowledgement

The authors are grateful to Micronet, Networks of Centres of Excellence Program, and Natural Science and Engineering Research Council of Canada, for supporting this work. Programming assistance provided by C. M. Leung is also greatly appreciated.


## References


[1] G. Karlsson and M. Vetterli, "Theory of two dimensional multirate filter banks," *IEEE Trans. Acous., Speech, Signal Processing*, vol. 38, pp. 925–937, June 1990.

[2] E. Viscito and J. P. Allebach, "The analysis and design of multidemensional FIR perfect reconstruction filter banks for arbitrary sampling lattices," *IEEE Trans. Circuits Syst.*, vol. 38, pp. 29–41, Jan. 1991.

[3] R. Ansari, H. P. Gaggioni, and D. J. LeGall, "HDTV coding using a nonrectangular subband decomposition," in *Proc. SPIE Visual Communication and Image Processing' 88*, vol. 1001, pp. 821–825, 1988.

[4] M. Vetterli, J. Kovacevic, and D. LeGall, "Perfect reconstruction filter banks for HDTV representation and coding," in *Proc. 3rd Int. Workshop on HDTV*, Torino, 1989.

[5] T. Chen and P. P. Vaidyanathan, "Multidimensional multirate filters and filter banks derived form one dimensional filters," *IEEE Trans. Signal Processing*, vol. 41, pp. 1749–1765, May 1993.

[6] T. Chen and P. P. Vaidyanathan, "Recent development in multidimensional multirate systems," *IEEE Trans. Circuits Syst.:Video Technology*, vol. 3, pp. 116–137, April 1993.

[7] D. B. H. Tay and N. G. Kingsbury, "Flexible design of multidimensional perfect reconstruction FIR 2 band filters using transformations of variables," *IEEE Trans. Image Processing*, vol. 2, pp. 466–481, Oct. 1993.

[8] V. Ouvrard and P. Siohan, "Design of two dimensional non separable QMF banks," in *Proc. IEEE Int. Conf. Acoust, Speech, Signal Processing*, vol. IV, pp. 645–648, April 1992.

[9] C. K. Chen and J. H. Lee, "Design of quadrature mirror filters with linear phase in the frequency domain," *IEEE Trans. Circuits Syst. II*, vol. 39, pp. 593–605, Sept. 1992.

[10] H. Xu, W. S. Lu, and A. Antoniou, "Improved iterative methods for the design of quadrative mirror image filter banks," *IEEE Trans. Circuits Syst.*, vol. 43, pp. 363–371, May 1996.

[11] H. Xu, W. S. Lu, and A. Antoniou, "Efficient iterative design method for cosine modulated QMF banks," *IEEE Trans. Signal Processing*, vol. 44, pp. 1657–1668, July 1996.

[12] D.G. Luenberger, *Linear and Nonlinear Programming*, 2nd ed., Reading, MA: Addison Wesley, 1984.

[13] W. S. Lu and A. Antoniou, *Two Dimensional Digital Filters*, New York: Marcel Dekker, 1992.

[14] A. Ostrowski, *Solution of Equations in Euclidean and Banach Spaces*, 3rd ed., New York: Academic Press, 1973.